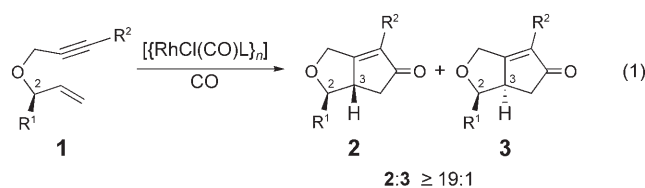


# Mechanistic Insight into the Diastereoselective Rhodium-Catalyzed Pauson–Khand Reaction: Role of Coordination Number in Stereocontrol\*\*

Huijun Wang, James R. Sawyer, P. Andrew Evans,\* and Mu-Hyun Baik\*

Transition-metal-catalyzed higher-order  $[m+n+o]$  carbocyclization reactions represent powerful methods for the construction of complex polycyclic systems.<sup>[1]</sup> A key feature in these transformations is the dichotomy in reactivity that a substrate will display with different transition-metal complexes, reminiscent of enzyme-directed terpene biosynthesis.<sup>[2]</sup> Although catalyst-controlled reactions are very well established, they are generally identified empirically rather than through the ability to a priori select the optimal catalyst for a particular transformation. DFT calculations have emerged as a powerful predictive tool capable of aiding the design and understanding of these types of reactions and their application to challenging synthetic problems.<sup>[3]</sup> Herein, we demonstrate theoretically the impact of coordination number on the level of diastereocontrol in the rhodium-catalyzed Pauson–Khand (PK) reaction [Eq. (1)] and experimentally support the hypothesis.<sup>[4]</sup>



Initial computational studies focused on the examination of the rhodium-catalyzed PK reaction of functionalized 1,6-enyne **1** with carbon monoxide in the context of the diastereoselective formation of the bicyclopentenones **2** and **3** [Eq. (1)]. At the outset of this study, we sought to address the following objectives: 1) determine the composition of the active catalytic species, 2) provide an accurate model for stereocontrol, and 3) understand the role of spectator ligands on the metal center. Although we had demonstrated that excellent diastereoselectivity could be obtained using various rhodium catalysts of the general type  $[\{\text{RhCl}(\text{CO})\text{L}_n\}]$  (where  $n=1, 2$  and  $\text{L}=\text{PPh}_3$ , 1,2-bis(diphenylphosphanyl)ethane (dppe), etc.),<sup>[5]</sup> we elected to examine simpler complexes that lacked the phosphine ligands to garner a deeper understanding of their influence on selectivity.<sup>[6–11]</sup>

The origin of stereocontrol had originally been rationalized by invoking facially selective metal binding, which was envisioned to originate from steric demands imposed by the substituent at the C2 stereogenic center.<sup>[5]</sup> To accurately probe and fully understand the origin of the selectivity in greater detail, we utilized high-level density functional methods at the B3LYP/cc-pVTZ(-f)<sup>[12,13]</sup> level of theory implemented in the numerically efficient program package Jaguar,<sup>[14]</sup> which allowed us to explore a large number of possible structural isomers and reaction pathways.<sup>[15]</sup> Mechanistically, the cyclization is generally accepted to occur through the initial formation of a  $\pi$  complex, which then undergoes oxidative addition, migratory insertion of CO, and reductive elimination to regenerate the rhodium(I) catalyst and afford the cyclopentenone. Interestingly, we discovered that the relationship between the metal complex and stereocontrol is much more complex than had previously been envisioned.

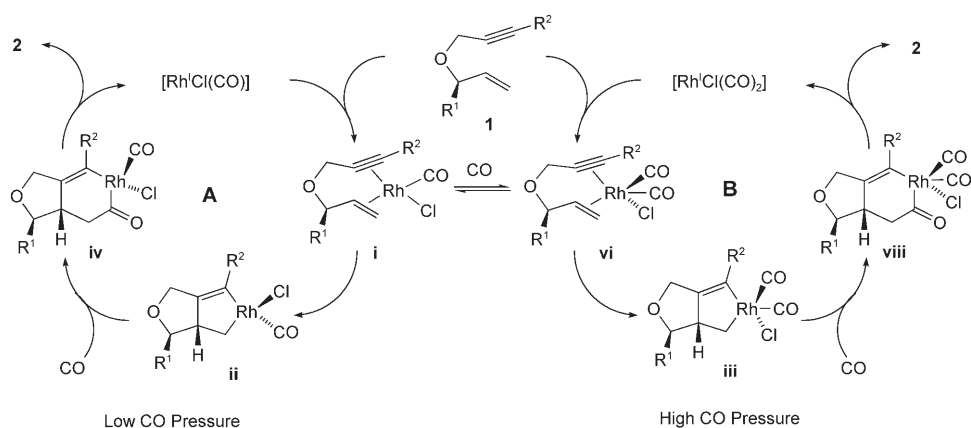
A critical obstacle in the construction of a theoretical model for the rhodium-catalyzed PK reaction was that the exact composition of the catalytically competent rhodium complex was unknown. Hence, we envisioned probing this relationship with  $[\text{Rh}^{\text{I}}\text{Cl}(\text{CO})]$  and  $[\text{Rh}^{\text{I}}\text{Cl}(\text{CO})_2]$ , which should form  $\pi$  complexes with the 1,6-enyne to afford an approximately square-planar 16-electron complex **i** and a trigonal-bipyramidal 18-electron complex **vi**, respectively (Scheme 1).<sup>[3]</sup> Exploration of the complete reaction pathways using both possibilities determined that each of these pathways is mechanistically relevant. Figure 1 illustrates the computed solution-phase free-energy reaction profiles using  $[\text{Rh}^{\text{I}}\text{Cl}(\text{CO})]$  as the catalytically competent species. Upon formation of the  $\pi$  adduct **i**, oxidative addition affords one of two possible diastereomeric metallacycles **ii** and **ii'**, in which

[\*] Prof. P. A. Evans  
Department of Chemistry, The University of Liverpool  
Liverpool, L69 7ZD (UK)  
Fax: (+44) 151-794-1377  
E-mail: Andrew.Evans@liverpool.ac.uk  
Homepage: <http://osxs.ch.liv.ac.uk/>

Prof. M.-H. Baik  
Department of Chemistry and School of Informatics  
Indiana University  
800 E. Kirkwood Avenue, Bloomington, IN 47405 (USA)  
Fax: (+1) 812-856-0454  
E-mail: mbaik@indiana.edu  
Homepage: <http://baik.chem.indiana.edu/>

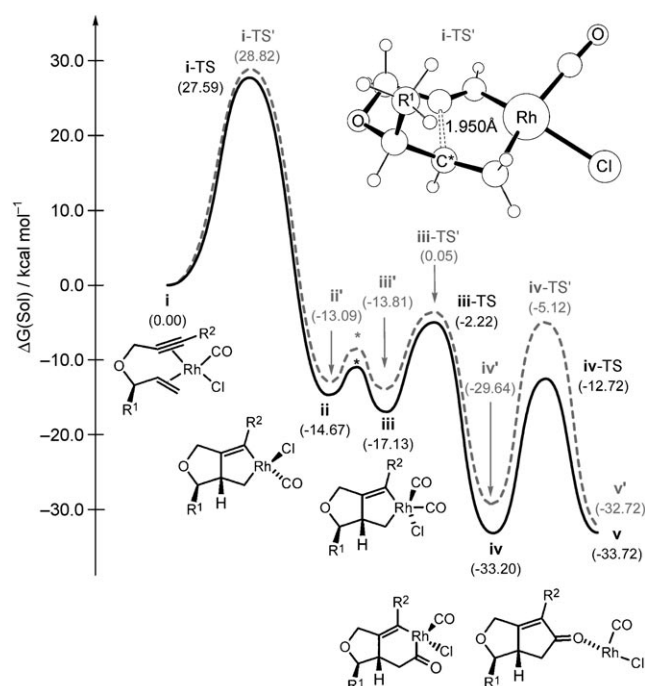
H. Wang, J. R. Sawyer  
Department of Chemistry, Indiana University  
Bloomington, IN 47405 (USA)

[\*\*] We thank the NIH (HG003894 and GM58877) and NSF (0116050 and CHE-0645381) for financial support. We also thank the Royal Society for a Wolfson Research Merit Award (P.A.E.), the Research Corporation for a Cottrell Award (M.H.B.), the Sloan Foundation for a Sloan Fellowship (M.H.B.), and Eli Lilly for sponsorship of a Graduate Fellowship (J.R.S.).

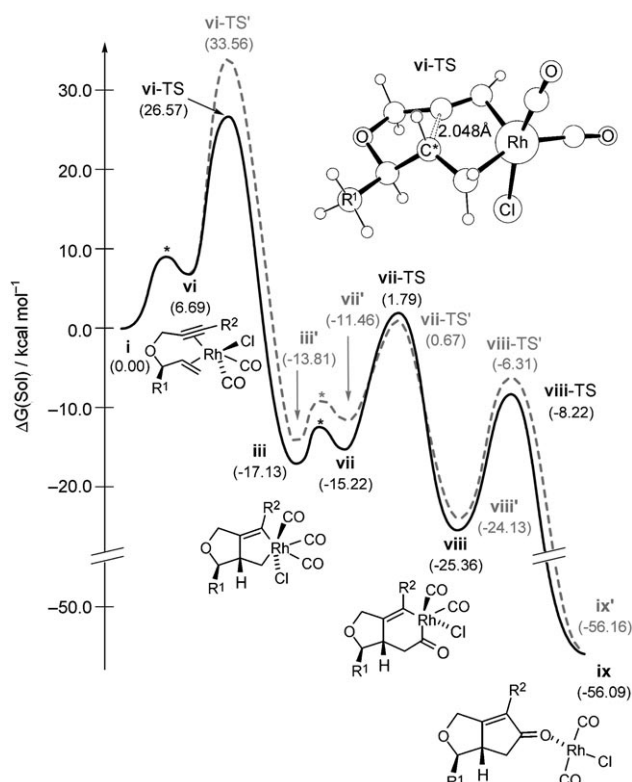


Scheme 1.

Surprisingly, the rate-determining transition states of the two possible reaction pathways are found to be highly sensitive to the presence of an additional carbonyl ligand on the rhodium center. Figure 2 illustrates the reaction energy profiles for the addition of a carbonyl ligand to the initial reactant complex **i** to afford the five-coordinate 18-electron complex **vi**, which is energetically disfavored by 6.7 kcal mol<sup>-1</sup> owing to the weakening of the rhodium–


 Figure 1. Reaction energy profile utilizing  $[\text{RhCl}(\text{CO})]$  as the catalytically active species.

the C3 hydrogen atom is either *syn* or *anti* to  $\text{R}^1$ , respectively. Addition of a CO ligand gives complexes **iii** and **iii'**, which undergo migratory insertion to give the six-membered metalacycles **iv** and **iv'** after traversing the non-rate-limiting transition states **iii-TS** and **iii-TS'**. Reductive elimination finally furnishes the product complexes **v** and **v'**. The reaction pathway leading to diastereomer **2** is associated with a solution-phase activation free energy of 27.6 kcal mol<sup>-1</sup> (**i-TS** in Figure 1), whereas the transition state **i-TS'** that ultimately yields product **3** is computed to be only 1.2 kcal mol<sup>-1</sup> higher in energy. This energy difference predicts the upper limit of the diastereomeric ratio (d.r.) to be approximately 10:1, which is too small to explain the observed level of diastereocontrol.


 Figure 2. Reaction energy profile utilizing  $[\text{RhCl}(\text{CO})_2]$  as the catalytically active species.

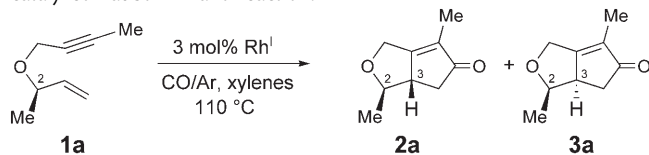
enyne interaction and loss of entropy upon carbonyl binding. As the metal center accepts  $\sigma$  electron density from the additional CO ligand, the antibonding interaction of the now five-coordinate rhodium complex with the original substrate becomes more pronounced. The different energy components are enumerated in the Supporting Information. The axial addition of the carbonyl ligand to the pseudo-square-planar rhodium center forces the chlorido ligand to be *trans* to the axial CO ligand in **vi**. The presence of the second carbonyl ligand increases the overall reaction rate slightly, with the energy of the new transition state **vi-TS** being 26.6 kcal mol<sup>-1</sup>. Interestingly, the additional carbonyl ligand has the opposite

effect on the reaction pathway that gives rise to the diastereomeric analogue **3** and increases its barrier to 33.6 kcal mol<sup>-1</sup>, which is too high to give any reaction under the prescribed reaction conditions. Hence, the calculations predict high levels of diastereoselectivity only if the catalytically active species is the trigonal-bipyramidal adduct.

At an energetic difference to **i** of 6.7 kcal mol<sup>-1</sup>, intermediate **vi** is thermodynamically not preferred. The equilibrium between **i** and **vi**, however, is highly dependent on the CO concentration. At relatively high CO concentrations, the most prevalent species will be **vi**, while **i** is expected to be the dominant species at low CO concentration. Thus, our calculations predict a substantial loss in diastereoselectivity when the CO concentration is lowered, owing to a shift of the equilibrium in favor of **i**. Note that our molecular calculations assume a 1:1 stoichiometry of **i** and CO for the formation of **vi**. Because we are able to quantify neither the concentration of the catalytically active Rh species nor that of CO in solution, we are unable to correct our idealized simulated energies for standard states. However, it is clear that the energy of the transition state **vi**-TS is an upper-limit estimate and would be a few kilocalories per mole lower if the concentration differentials could be considered. The computed rate-determining barriers for the four-coordinate Rh catalyst do not suffer from the pre-equilibrium condition. Thus, our calculations suggest that the energy difference between the lowest barrier for forming **2a** and **3a** ( $R^1 = R^2 = \text{Me}$ ) is at least (but likely larger than) 2.25 kcal mol<sup>-1</sup>, thus suggesting a d.r. larger than 100:1 in favor of **2a** under high CO pressure.

To challenge this theoretical hypothesis, the reaction was performed with varying compositions of argon and carbon monoxide to alter the equilibrium ratio. Table 1 summarizes the results from this study, which provides compelling evidence in support of our prediction. For example, while the PK reaction at high CO concentration proceeded with excellent diastereoselectivity (Table 1, entry 1), the reactions at 10% and 5% CO furnished the bicyclic products **2a** and **3a**

**Table 1:** Effect of CO pressure on the diastereoselectivity of the rhodium-catalyzed Pauson–Khand reaction.<sup>[a]</sup>



Entry	Rhodium complex	Pressure [atm]		Yield [%] <sup>[b]</sup>	d.r. <sup>[c]</sup> <b>2a</b> : <b>3a</b>
		CO	Ar		
1	{[RhCl(CO) <sub>2</sub> ] <sub>2</sub> }	1.00	0.00	81	22:1
2	{[RhCl(CO) <sub>2</sub> ] <sub>2</sub> }	0.10	0.90	64	10:1
3	{[RhCl(CO) <sub>2</sub> ] <sub>2</sub> }	0.05	0.95	57	6:1
4	{[RhCl(CO)(dppp)] <sub>2</sub> } <sup>[d]</sup>	1.00	0.00	88	≥ 99:1
5	{[RhCl(CO)(dppp)] <sub>2</sub> }	0.10	0.90	51	58:1
6	{[RhCl(CO)(dppp)] <sub>2</sub> }	0.05	0.95	44	57:1

[a] All reactions were carried out on a 0.25 mmol reaction scale utilizing 3 mol% of the rhodium complex in xylene at 110 °C. [b] Yields of isolated product. [c] Ratios of diastereoisomers were determined by capillary GLC analysis on the crude reaction mixtures. [d] dppp = 1,3-bis(diphenylphosphanyl)propane.

with significantly diminished diastereomeric ratios of 10:1 and 6:1 respectively (Table 1, entries 2 and 3).<sup>[16]</sup>

In light of the experimental findings, we were prompted to question why the additional carbonyl ligand has such a decisive impact on the two reaction pathways. An intuitive rationale emerges by considering the two transition states illustrated in Figures 1 and 2. In **i**-TS and **i**-TS', the reactive rhodium center adopts an approximately square-planar geometry in which the  $\pi$ -donating chlorido ligands increase the polarizability of the metal-centered electron density in the molecular plane. As a result, the rhodium center is highly reactive towards oxidative addition when the metallacycle is formed in the molecular plane. Addition of carbonyl as the fifth ligand, on the other hand, forces the chlorido group into the axial position in order to maximize the push-and-pull resonance in the  $\pi$  space along the linear Cl-Rh-CO axis. Thus, the rhodium center is less electron-rich, and structural differences translate into larger energy differences of the transition state, as the correct molecular orbitals have to align properly to promote oxidative addition, thus leading to higher selectivity.<sup>[17]</sup> This analysis implies that the trigonal-bipyramidal coordination geometry of rhodium is generally preferable for promoting stereoselective carbocyclizations. Hence, the presence of strongly binding spectator ligands, such as phosphines, are likely to enforce a trigonal-bipyramidal geometry and thereby afford high levels of diastereoselectivity, regardless of CO pressure. We were able to confirm this prediction experimentally, as outlined in Table 1 (entries 4–6), which thereby further supports the original theoretical prediction. The lower overall efficiency of the transformations at lower CO pressure may be attributed to the catalyst promoting alternative reaction pathways (Table 1, entries 5,6).

In summary, we have demonstrated that theoretical analysis of the rhodium-catalyzed PK reaction provides two mechanistic scenarios for the origin of diastereoselectivity, in which optimum selectivity can be attributed to a five- rather than a four-coordinate organorhodium complex. The relative population of these complexes is related to carbon monoxide concentration, which contrasts the phosphine-containing rhodium(I) complexes that preferentially adopt a 5-coordinate configuration irrespective of the amount of carbon monoxide present. Finally, this work serves to highlight how an intuitive mechanistic scenario, such as the applied CO pressure being a controlling factor for the stereochemical outcome of the PK reaction, may be predicted and experimentally verified.

Received: June 26, 2007

Revised: August 7, 2007

Published online: November 19, 2007

**Keywords:** carbocyclization · density functional calculations · diastereoselectivity · homogeneous catalysis · rhodium

[1] For recent reviews of transition-metal-catalyzed carbocyclization reactions, see: a) C. Aubert, O. Buisine, M. Malacria, *Chem. Rev.* **2002**, *102*, 813–834; b) *Modern Rhodium-Catalyzed Organic Reactions* (Ed.: P. A. Evans), Wiley-VCH, Weinheim,

- 2005; c) C. Aubert, L. Fensterbank, V. Gandon, M. Malacria, *Top. Organomet. Chem.* **2006**, *19*, 259–294.
- [2] For a recent review on the structural biology and chemistry of terpenoid cyclases, see: D. W. Christianson, *Chem. Rev.* **2006**, *106*, 3412–3442.
- [3] For recent examples of DFT calculations on rhodium-catalyzed higher-order carbocyclization reactions, see: a) Z.-X. Yu, P. A. Wender, K. N. Houk, *J. Am. Chem. Soc.* **2004**, *126*, 9154–9155; b) M.-H. Baik, E. W. Baum, M. C. Burland, P. A. Evans, *J. Am. Chem. Soc.* **2005**, *127*, 1602–1603.
- [4] For recent reviews of Pauson–Khand type reactions, see: a) N. Jeong in *Modern Rhodium-Catalyzed Organic Reactions* (Ed.: P. A. Evans), Wiley-VCH, Weinheim, **2005**, pp. 215–240; b) T. Shibata, *Adv. Synth. Catal.* **2006**, *348*, 2328–2336; c) J. Perez-Castells, *Top. Organomet. Chem.* **2006**, *19*, 207–257.
- [5] P. A. Evans, J. E. Robinson, *J. Am. Chem. Soc.* **2001**, *123*, 4609–4610.
- [6] For an example of an allene–ene PK reaction using  $[[\text{RhCl}(\text{CO})_2]_2]$ , see: F. Inagaki, C. Mukai, *Org. Lett.* **2006**, *8*, 1217–1220.
- [7] For an example of allene–yne PK reactions using  $[[\text{RhCl}(\text{CO})_2]_2]$ , see: a) C. Mukai, I. Nomura, K. Yamanishi, M. Hanaoka, *Org. Lett.* **2002**, *4*, 1755–1758; b) K. M. Brummond, H. Chen, K. D. Fisher, A. D. Kerekes, B. Rickards, P. C. Still, S. J. Geib, *Org. Lett.* **2002**, *4*, 1931–1934.
- [8] For examples of enyne PK reactions with  $[[\text{RhCl}(\text{CO})_2]_2]$ , see: a) Y. Koga, T. Kobayashi, K. Narasaka, *Chem. Lett.* **1998**, 249–250; b) T. Kobayashi, Y. Koga, K. Narasaka, *J. Organomet. Chem.* **2001**, *624*, 73–87.
- [9] For examples of diene–ene PK reactions, see: a) S. I. Lee, J. H. Park, Y. K. Cheung, S.-G. Lee, *J. Am. Chem. Soc.* **2004**, *126*, 2714–2715; b) P. A. Wender, M. P. Croatt, N. M. Deschamps, *J. Am. Chem. Soc.* **2004**, *126*, 5948–5949; c) P. A. Wender, N. M. Deschamps, T. J. Williams, *Angew. Chem.* **2004**, *116*, 3138–3141; *Angew. Chem. Int. Ed.* **2004**, *43*, 3076–3079.
- [10] For an example of a diene–yne PK reaction using  $[[\text{RhCl}(\text{CO})_2]_2]$ , see: M.-C. P. Yeh, W.-C. Tsao, J.-S. Ho, C.-C. Tai, D.-Y. Chiou, L.-H. Tu, *Organometallics* **2004**, *23*, 792–799.
- [11] For an example of a sequential alkylation/PK reaction using  $[[\text{RhCl}(\text{CO})_2]_2]$ , see: B. L. Ashfeld, K. A. Miller, A. J. Smith, K. Tran, S. F. Martin, *Org. Lett.* **2005**, *7*, 1661–1663.
- [12] a) A. D. Becke, *J. Chem. Phys.* **1993**, *98*, 5648–5652; b) A. D. Becke, *Phys. Rev. A* **1988**, *38*, 3098–3100.
- [13] C. T. Lee, W. T. Yang, R. G. Parr, *Phys. Rev. B* **1988**, *37*, 785–789.
- [14] Jaguar 6.0, Schrödinger, Inc., Portland, Oregon, **2003**.
- [15] See the Supporting Information.
- [16] Note that our computational study uses a slightly simplified model ( $\text{R}^2 = \text{H}$ ) compared to the experimental work ( $\text{R}^2 = \text{CH}_3$ ). The stationary points of the potential-energy surface were re-evaluated with the methyl group, and we found no meaningful differences. We also evaluated experimentally the  $\text{R}^2 = \text{H}$  case and varied the substrate to contain nitrogen and carbon linker moieties, which were previously identified as common substrates for PK reactions. We found the same trend discussed for the model system, although the yield and diastereoselectivity were generally lower. These results are summarized in the Supporting Information.
- [17] A full electronic structure analysis detailing the molecular orbitals that are responsible for this different behavior will be presented in greater detail elsewhere.